ISSN 1064-2307, Journal of Computer and Systems Sciences International, 2015, Vol. 54, No. 3, pp. 415–423. © Pleiades Publishing, Ltd., 2015.
Original Russian Text © V.E. Vavilov, R.A. Gaisin, A.A. Gerasin, F.R. Ismagilov, I.Kh. Khairullin, 2015, published in Izvestiya Akademii Nauk. Teoriya i Sistemy Upravleniya, 2015, No. 3, pp. 88–96.

CONTROL SYSTEMS FOR TECHNOLOGICAL PROCESSES

Sensorless Control of Hybrid Magnetic Bearings

V. E. Vavilov, R. A. Gaisin, A. A. Gerasin, F. R. Ismagilov, and I. Kh. Khairullin

Ufa State Aviation Technical University, Ufa, Russia

e-mail: S2_88@mail.ru

Received January 13, 2014; in final form, October 10, 2014

Abstract—A method of sensorless rotor position control in noncontact bearings by output parameters of the electromechanical energy converter is proposed. The physical essence of the method is as follows. As the displacement of an electromechanical energy converter rotor along the axes x and y varies, the conductivity of the air gap and, accordingly, of the magnetic conductivity of the air gap changes; i.e., in the case of the rotor displacement, additional harmonic components of the magnetic induction occur that create additional harmonic components of the electromotive force. The estimation of these harmonic components makes it possible to determine the displacement of the rotor without the use of rotor position sensors. The mathematical apparatus and the sensorless rotor position control algorithm based on this apparatus have been developed for practical implementation of the proposed method.

DOI: 10.1134/S1064230715020124

INTRODUCTION

The particular emphasis in the development of control systems for hybrid magnetic bearings (HMB) of electromechanical energy converters (EMEC) is made on rotor position sensors (RPSs), whose main task is the highly accurate measurement of rotor displacement in time [1]. Requirements for rotor position sensors (high precision and maximum performance at minimum weight-size parameters and maximum reliability) determine their cost, which can be up to 30–50% of the cost of all the HMB as a whole [2]. A number of companies, such as *Ebara Corporation* [3, 4], develop sensorless control systems for active magnetic bearings (AMB) in order to solve these problems. There are no RPSs in these systems, and the rotor displacement is estimated by the change in inductance or impedance of electromagnets of AMBs in the case of rotor displacement. It is important to note that the accuracy of the rotor position control and operability of such systems are largely affected by the thermal processes occurring within EMECs, which affect the resistance of electromagnets and, therefore, their inductance and impedance. In addition, such control systems must have their own control unit that has significant weight and size parameters, which usually reduce the efficiency of not only sensorless systems but also all magnetic bearings in general.

Therefore, a relevant and important scientific task is to develop sensorless control systems for hybrid magnetic bearings which are almost not affected by thermal processes in EMECs. The solution to this problem will significantly reduce weight and size parameters of EMECs on HMBs (because of the integration of the HMB control system into functional systems of EMECs) and costs of the development and operation of EMECs based on HMB (because there will be no rotor position sensors), as well as improve control accuracy and reliability of EMECs.

1. FORMULATION OF THE PROBLEM

The novel method for determining the rotor position in sensoreless bearings based on the output EMEC parameters can provide a solution to this problem. The physical essence of this method is as follows: the displacement of the EMEC rotor the axes x and y, the conductivity of the air gap changes, which leads to a change in the magnetic field in the air gap of the EMEC; i.e., as the rotor is displaced, additional harmonic components of the magnetic induction occur in the air gap [5]; these are

(1) harmonics with $p \pm n$ pole pairs (where $n = 1, 2, 3...$ and p is number of rotor pole pairs) and the order $1 \pm p/n$ caused by components of the magnetic conductance.

(2) The higher harmonics with $p \pm n \pm kZ$ pole pairs of and the order $1 \pm n/p \pm kZ/p$ (where $k = 1, 2, 3 ...$, Z is the number of stator teeth).

Qualitative comparative analysis of conventional (sensor) control methods, sensorless methods developed by *Simens* and *Ebara Corporation*, and the proposed method

Comparison criterion	Conventional control methods using displacement sensors	Known sensorless control methods for changing the impedance or inductance of electromagnets	Proposed sensorless control method
Weight and size parameters	High. Sensors require additional space for installation inside the EMEC casing	It becomes possible to reduce the weight and size of the EMEC	It becomes possible to reduce the weight and size of the EMEC
Price characteristics	High due to sensor prices	Low because there are no rotor position sensors	Low because there are no rotor position sensors
Possibility of integration into EMEC functional systems	There are a number of difficulties because of the need to modernize and complicate the functional diagnostics systems	Integration with EMEC functional systems is difficult because the control system is intended only for the rotor position determination	Output current and voltage are measured in EMEC functional systems; therefore, there are no major problems for the integration
Reliability	Low due to both the presence of the sensors themselves and the need to feed them with an extra cable	There is an opportunity to improve reliability	There is an opportunity to improve reliability
Energy efficiency	Low because in some cases sensors require an additional power supply	Higher	Higher
Sensitivity to external influences	High because sensors are thermal and vibration proof	Low because the characteristics of control system electromagnets depend both on the temperature inside the EMEC casing and on rotor vibrations	High since the characteristics are determined directly from EMEC parameters and can be adjusted depending on the EMEC state
The use in various structural modifications of HMBs	Can be used in all structural modifications	Only in modifications with electromagnets	Can be used in all structural modifications

These harmonic components of the magnetic field in the air gap will manifest themselves in the electromotive force (EMF) and voltage created by this field. Then, their presence and absolute magnitude can be used to determine the displacement of the rotor of EMECs based on HMBs and to control this displacement using either an electromagnet or nozzle. At the same time, these harmonic components are measured in the normal EMEC operation mode, i.e., when the temperature of EMEC windings reached a steady state and can only be changed in EMEC emergency operation modes, such as short-circuit. Thus, the proposed method is resistant to thermal processes in EMECs. In other words, if the temperature of EMEC windings is 120°C and the winding resistance is 0.003 Ω, then the temperature change by more than 10% will indicate the EMEC failure, and the change of less than 10% will not significantly affect the harmonic components because the resistance will change only by 3–5%. The table provides a qualitative comparative analysis of conventional (sensor) control methods, sensorless methods developed by *Simens* and *Ebara Corporation*, and the proposed method.

Thus, the table shows that the proposed sensorless control method has several advantages over both known sensorless control methods and conventional systems. Therefore, it has promising practical applications.

For the practical implementation of the proposed method, it is necessary to develop a mathematical apparatus that describes the relationship of EMEC output parameters on rotor displacement. In this case, a high-speed permanent magnet generator (HSPMG) on HMBs is considered as an EMEC (Fig. 1).

In solving this problem, the following assumptions are made:

(1) The magnetic permeability throughout the whole region between the stator and the rotor equals the vacuum permeability, the magnetic permeability of the permanent magnets is constant, and the magnetic permeability of the stator iron is infinite.

(2) The HSPMG operates in the symmetric steady state.

(3) The inductive reactance along the axis q equals the inductive reactance along the axis d.

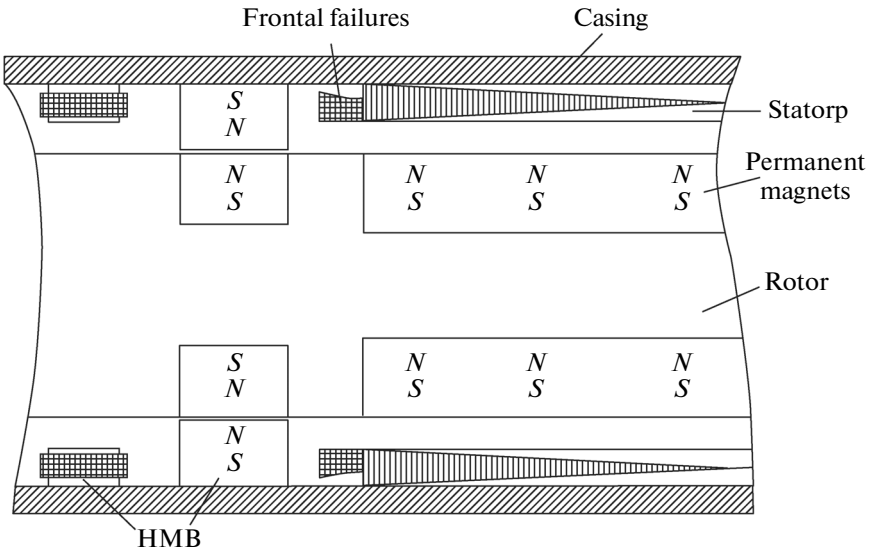

Fig. 1. HSPMG based on HMB.

These assumptions are standard for this class of problems and do not introduce significant errors, while the effect of some of them can be accounted for individually; for example, the saturation of the stator iron is taken into account by the introduction of the saturation coefficient.

2. MATHEMATICAL DESCRIPTION OF THE PLANT

Given the assumption of the equality of inductive reactances along the axes d and q, the electromechanical energy conversion in the HSPMG is described by the system of equations (see [6])

$$\begin{aligned}
&\frac{d}{dt}i_d = \frac{1}{L_d}u_d - \frac{r_a}{L_d}i_q + \frac{L_q}{L_d}p\omega i_q,\\
&\frac{d}{dt}i_q = \frac{1}{L_q}u_q - \frac{r_a}{L_q}i_q + \frac{L_d}{L_q}p\omega i_d - \frac{p\omega\psi}{L_q},\\
&M_e = 1.5p\psi i_q,\\
&\frac{d}{dt}\omega = \frac{1}{J}(M_{\mathrm{M}} - k_{\mathrm{fr}}\omega - M_e),
\end{aligned} \tag{2.1}$$

where i_d, i_q are the projections of currents on the axes q and d; u_d, u_q are the projections of voltages applied to the stator on the axes q and d; L_d, L_q are the inductances on the axes d and q; p is the number of pole pairs of the HSPMG; ω is the rotor rotation rate; ψ is the phase stator flux linkage; M_{M} is the mechanical torque of the drive; k_{fr} is the coefficient taking into account the friction in the bearings; J is the moment of inertia; M_e is the electromagnetic moment; and r_{a} is the HSPMG ohmic resistance.

The inductive reactance of the stator winding in the transverse or longitudinal axis for non-salient pole HSPMG is determined by the sum [7]

$$x_d = x_{\mathrm{a}} + x_{\sigma}, \tag{2.2}$$

where x_{a} is the inductive resistance of the stator winding and x_{σ} is the leakage reactance.

The inductive reactance of the stator winding if there is no rotor displacement is

$$x_{\mathrm{a}} = \frac{4\mu_0 mf\left(wk_{\mathrm{w}}\right)^2\tau l}{\pi p k_{\delta}\delta}, \tag{2.3}$$

where m is the number of phases of the HSPMG; f is the current frequency in the HSPMG windings; w is the number of turns; δ is the HSPMG air gap; l is the active length of the stator pack; k_{w} is the winding

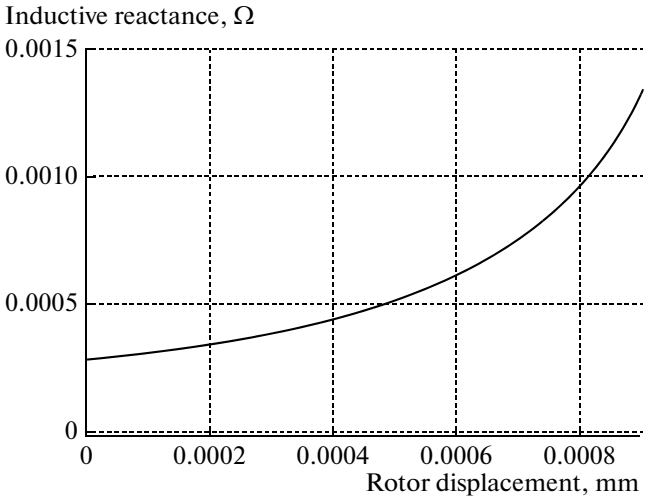

Fig. 2. The dependence of the inductance on the rotor displacement.

ratio; τ is the pole pitch of the HSPMG rotor; μ_0 is the magnetic permittivity of vacuum; k_δ is the coefficient taking into account the stator slotting; and p is the number of HSPMG pole pairs.

In the case of the radial rotor displacement, the HSPMG air gap will vary according to the law

$$\delta = \delta_0 - x\cos\alpha - y\sin\alpha, \tag{2.4}$$

where δ_0 is the nominal air gap of the HSPMG; x and y is the rotor displacement in the Cartesian coordinate system; and α is the rotor angular coordinate.

Then, the stator inductive reactance in the case of the HSPMG rotor displacement with regard to (2.4) will be

$$x_a = \frac{4\mu_0 mf\left(wk_w\right)^2 \tau l}{\pi p k_\delta \left(\delta_0 - x\cos\alpha - y\sin\alpha\right)}. \tag{2.5}$$

The leakage reactance depends on the leakage conductivity coefficients and is determined by the known relation

$$x_\sigma = 15.8\frac{f}{100}\left(\frac{w}{100}\right)^2 \frac{l}{pq_m}\left(\lambda_s + \lambda_e + \lambda_d\right), \tag{2.6}$$

where λ_s, λ_e, and λ_d are the coefficients of the slot, end, and differential specific leakage conductivity, respectively; q_m is the number of slots per pole and phase; and p is the number of HSPMG pole pairs.

The specific conductivity coefficients of slot and end leakages are determined by the geometric parameters of the slot, coil ends, and properties of isolation; however, they are independent of the air gap changes. Taking into account (2.4), the coefficient of the specific differential leakage conductivity can be written as

$$\lambda_d = 0.03\frac{\tau\alpha_i}{\left(\delta_0 - x\cos\alpha - y\sin\alpha\right)k_\delta q}, \tag{2.7}$$

where α_i is the pole overlap ratio. Then

$$L_d = L_q = \frac{1}{f}\left[\frac{4\mu_0 mf\left(wk_w\right)^2 \tau l}{\pi p k_\delta \left(\delta_0 - x\cos\alpha - y\sin\alpha\right)} + 15.8\frac{f}{100}\left(\frac{w}{100}\right)^2 \frac{l}{pq}\left(\lambda_s + \lambda_e + 0.03\frac{\tau\alpha_i}{\left(\delta_0 - x\cos\alpha - y\sin\alpha\right)k_\delta q_m}\right)\right]. \tag{2.8}$$

Figure 2 shows the dependence of the inductance along the axes d and q on the rotor displacement for the HSPMG with the rotation rate of 12000 rpm, power of 100 kW, four turns, and the air gap per side of 1 mm.

It can be seen from the analysis of Fig. 2 that if the rotor displacement increases by 90% of the air-gap, then the inductances along the axes d and q increase by a factor of 4.4. The air gap variation also affects the HSPMG flux linkage [8, 9] taking into account the fact that the HSPMG magnetomotive force is determined by the characteristics of used high-coercivity permanent magnets (HCPM): $F = H_c l$, where H_c is the HCPM coercivity; then,

$$\psi = \mu_0 w H_c l^2 \frac{2\tau}{\pi} \frac{1}{(\delta_0 - x\cos\alpha - y\sin\alpha)}. \tag{2.9}$$

According to (2.8), (2.9), and (2.1), a HSPMG mathematical model can be formulated that takes into account the rotor displacement in spatial coordinates.

3. PROBLEM SOLUTION

In real HSPMG operating conditions it is difficult to use voltages and currents in the two-phase coordinate system in order to determine the rotor displacement, as opposed, for example, to HMB brushless DC electric motors, where there is a control system in which currents and voltages are calculated in the two-phase coordinate system, and accordingly it becomes possible to design the motor control system and the HMB sensorless control system. The use of this approach in the HSPMG will lead to additional elements, which will greatly reduce efficiency obtained by solving the problem. In the HSPMG, it is most convenient to use the magnitudes that can be measured at output, i.e., voltage or electromotive force.

In [10, 11], by the interpolation of the experimental data using the least squares method, a generalized dependence of the first, third, ninth, and forty-third harmonic components of the output EMEC EMF on the static eccentricity was established:

$$\varepsilon = k_3 \Delta E_\nu^3 + k_2 \Delta E_\nu^2 + k_1 \Delta E_\nu + k_0; \tag{3.1}$$

here, k_1, k_2, k_3, k_0 are interpolation coefficients; $\Delta E_\nu = [(E_\nu - E_{\nu\text{сим}})/E_{\nu\text{сим}}] \cdot 100$ is the relative deviation of the measured EMF harmonics from the harmonic of the symmetric mode; $\varepsilon = [(\delta_{\max} - \delta_{\min})/(\delta_{\max} + \delta_{\min})] \cdot 100$ is the relative static eccentricity as a percentage of the nominal air gap; $\delta_{\max}, \delta_{\min}$ are the minimum and maximum air gaps in the case of the displacement; ν is the harmonic number; and $E_{\nu\text{sym}}$ are the harmonics of the symmetric mode (reference EMF).

The interpolation coefficients in Eq. (3.1) for the particular HSPMG are determined from the equation (see [8])

$$\sum_{l=0}^{3} k_l \int_0^{100} \varepsilon^{l+j-2} d\varepsilon = \int_0^{100} \varepsilon^{j-1} f(\varepsilon) d\varepsilon, \tag{3.2}$$

where $j = 1, \ldots, 4$ and $f(\varepsilon)$ is the function that describes the dependence of the rotor displacement on the EMF harmonics.

Then, by measuring the output EMF and representing it in the form of the harmonic series [9–11] it is possible to determine the static eccentricity of the rotor or its displacement from the condition

$$\begin{aligned} &k_{11}\Delta E_1^3 + k_{12}\Delta E_1^2 + k_{13}\Delta E_1 + k_{14} \approx k_{21}\Delta E_3^3 + k_{22}\Delta E_3^2 + k_{23}\Delta E_3 + k_{24} \\ &\approx k_{91}\Delta E_9^3 + k_{92}\Delta E_9^2 + k_{93}\Delta E_9 + k_{94} \approx k_{431}\Delta E_{43}^3 + k_{432}\Delta E_{43}^2 + k_{433}\Delta E_{43} + k_{434}. \end{aligned} \tag{3.3}$$

It follows from expression (3.3) that the magnitude of the eccentricity (rotor displacement) can be calculated only based on the harmonic 1 of the EMF, while the deviations of harmonics 3, 9, and 43 and, correspondingly, the magnitude of the eccentricity calculated on their basis are needed for the verification of the data obtained from the analysis of the first harmonic.

This method is of interest for systems of HSPMG functional diagnostics, but its use for sensorless control of the HMB rotor position is limited because the exact displacement coordinate and the trajectory of the HSPMG rotor are not known.

To accurately determine the displacement coordinate and the rotor motion trajectory, we introduce of the dependence of the measured value on the angular rotor coordinate; i.e., the EMF will be measured at predetermined rotor rotation angles (Fig. 3). For this purpose, the control elements ($P1$–Pk) (gas bearing

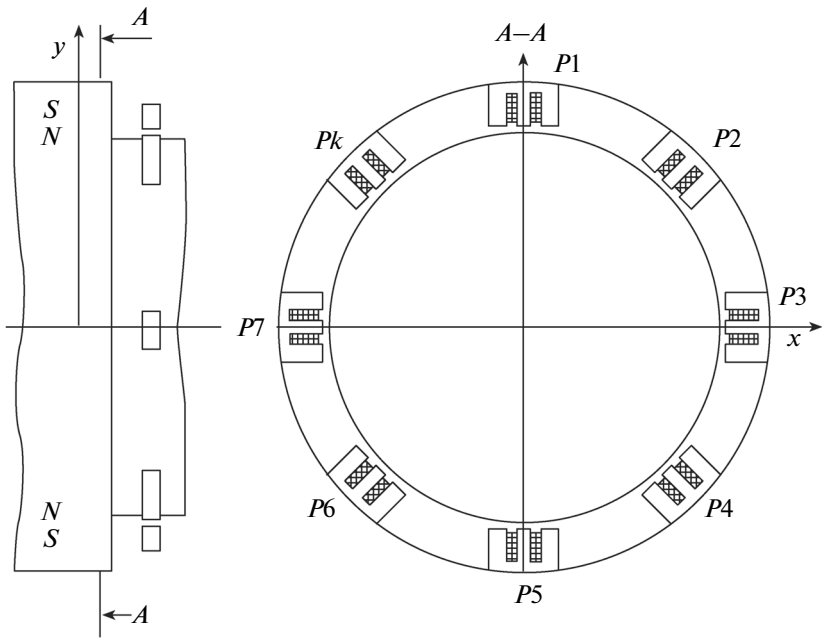

Fig. 3. To the determination of the HMB rotor position.

nozzles or electromagnet poles) are installed in the HSPMG casing in the direction specified by these angles.

Then, for the control element $P1$ with regard to expressions (3.1) and (3.2), we have

$$\begin{aligned}&\frac{(\delta_0 + y_{P1}) - (\delta_0 - y_{P1})}{(\delta_0 + y_{P1}) + (\delta_0 - y_{P1})} \approx k_{21}\Delta E_3^3(\varphi) + k_{22}\Delta E_3^2(\varphi) + k_{23}\Delta E_3(\varphi) + k_{24}\\ &\approx k_{91}\Delta E_9^3(\varphi) + k_{92}\Delta E_9^2(\varphi) + k_{93}\Delta E_9(\varphi) + k_{94}\\ &\approx k_{431}\Delta E_{43}^3(\varphi) + k_{432}\Delta E_{43}^2(\varphi) + k_{433}\Delta E_{43}(\varphi) + k_{434}.\end{aligned} \tag{3.4}$$

For $P2$, we obtain

$$\begin{aligned}&\frac{(\delta_0 + y_{P2}\cos 2\varphi + x_{P2}\sin 2\varphi) - (\delta_0 - y_{P2}\cos 2\varphi - x_{P2}\sin 2\varphi)}{(\delta_0 + y_{P2}\cos 2\varphi + x_{P2}\sin 2\varphi) + (\delta_0 - y_{P2}\cos 2\varphi - x_{P2}\sin 2\varphi)}\\ &\approx k_{21}\Delta E_3^3(2\varphi) + k_{22}\Delta E_3^2(2\varphi) + k_{23}\Delta E_3(2\varphi) + k_{24}\\ &\approx k_{91}\Delta E_9^3(2\varphi) + k_{92}\Delta E_9^2(2\varphi) + k_{93}\Delta E_9(2\varphi) + k_{94}\\ &\approx k_{431}\Delta E_{43}^3(2\varphi) + k_{432}\Delta E_{43}^2(2\varphi) + k_{433}\Delta E_{43}(2\varphi) + k_{434}.\end{aligned} \tag{3.5}$$

For Pk, we have

$$\begin{aligned}&\frac{(\delta_0 + y_{Pk}\cos k\varphi + x_{Pk}\sin k\varphi) - (\delta_0 - y_{Pk}\cos k\varphi - x_{Pk}\sin k\varphi)}{(\delta_0 + y_{Pk}\cos k\varphi + x_{Pk}\sin k\varphi) + (\delta_0 - y_{Pk}\cos k\varphi - x_{Pk}\sin k\varphi)}\\ &\approx k_{21}\Delta E_3^3(k\varphi) + k_{22}\Delta E_3^2(k\varphi) + k_{23}\Delta E_3(k\varphi) + k_{24}\\ &\approx k_{91}\Delta E_9^3(k\varphi) + k_{92}\Delta E_9^2(k\varphi) + k_{93}\Delta E_9(k\varphi) + k_{94}\\ &\approx k_{431}\Delta E_{43}^3(k\varphi) + k_{432}\Delta E_{43}^2(k\varphi) + k_{433}\Delta E_{43}(k\varphi) + k_{434},\end{aligned} \tag{3.6}$$

where y_{P1}, y_{P2}, x_{P2}, y_{Pk}, x_{Pk} are the rotor displacements at 1, 2, and k control element, respectively; k is the number of control elements; and $\varphi = 360/k$ is the angle of the EMF measurement and control location.

From these considerations it can be seen that in order to control the position of the rotor of the HMB HSPMG, it is necessary to know its angular coordinate and measure the output EMF. The angular coordinate can be determined by calculations (similarly to the sensorless vector control of the brushless motor [12]) or by setting one angle sensor, such as an encoder.

The sensorless control algorithm of the HMB by the EMF of the HSPMG can be formulated based on the developed mathematical apparatus.

4. ALGORITHM FOR CONTROLLING HYBRID MAGNETIC BEARINGS BY USING THE EXTERNAL MAGNETIC FIELD PATTERN

Let us consider the solution of this problem using a single-ring HMB with a control system as an example. The control system consists of eight electromagnets spaced equally along the perimeter of the HSPMG shaft (Fig. 3). The rotor rotation angle is determined by the encoder. In order to formalize the algorithm, the following notation is introduced: $P1$, $P2$, $P3$, $P4$, $P5$, $P6$, $P7$, and Pk are the electromagnets of the control system and *ef* is the encoder (not shown in Fig. 3).

(1) At the time of the HSPMG start, the voltage sensors measure the current EMF value at zero rotation angle (under electromagnet $P1$). The resulting EMF is decomposed into harmonic components [11]. The relative deviation of the EMF harmonics from the harmonics of the symmetric mode at zero angle is obtained.

(2) If the condition $\Delta E_1 > 2\%$ and (or) $\Delta E_3 > 2\%$, and (or) $\Delta E_9 > 2\%$ and (or) $\Delta E_{43} > 2\%$ holds, then the displacement under the considered electromagnet ($P1$) is determined as

$$y_{P1} \approx \left[k_{21}\Delta E_3^3 + k_{22}\Delta E_3^2 + k_{23}\Delta E_3 + k_{24}\right]\delta_0. \tag{4.1}$$

(3) If ΔE_1, ΔE_3, ΔE_9, $\Delta E_{43} > 0$, then the control signal is fed to the electromagnet $P1$ through the power amplifier, which causes the voltage increase in electromagnet windings and, correspondingly, the increase of the driving force. The proportional plus derivative control is used for the HMB rotor position. Its practical implementation is achieved by using the PD controller

$$I = \alpha y(P1) + \beta\frac{dy(P1)}{dt}, \tag{4.2}$$

where α, β are control factors that depend on the sum of the forces acting on the rotor and on HMB design features. In addition, the control coefficients α, β should be selected in such a way as to provide sustainable HMB rotor motion. The method of selecting these coefficients is described in [13].

(4) If ΔE_1, ΔE_3, ΔE_9, $\Delta E_{43} < 0$, then the control signal is fed to the electromagnet $P5$ through the power amplifier similarly to Step 3.

(5) According to encoder *ef* readings, the rotor rotation angle is determined, and the steps 1–3 are repeated for the angles 45, 90, 135, 180, 225, 270, and 315° and in the electromagnets ($P2$, $P3$, $P4$, $P5$, $P6$, $P7$, and $P8$) located in the direction of these angles.

5. NUMERICAL EXPERIMENT

The simulation model of HMB HSPMG was developed in order to verify the effectiveness of the proposed method. The model implements the proposed algorithm in Matlab Simulink. The block diagram of the simulation model is shown in Fig. 4.

The simulation model consists of the units HMB, HSPMG (the encoder is installed in the HSPMG), the unit that calculates the rotor displacement value, and the HMB control systems (HMB CS), in which the control is determined. The HSPMG unit was implemented according to equations (2.1). The flux linkage of the HSPMG was obtained from the rotor displacement (set in the HMB unit) using expression (2.9), and in the case of the concentric rotor position it was 0.12 Wb. In the numerical studies of the proposed algorithm, the HSPMG with the following parameters was considered: the inductance (L_d, L_q) along the axes d and q was 0.0242 Ω, there were eight poles, the power was 5 kW, the moment of inertia of the rotor was 0.0002102 kg/m^2, the rotation rate was 12000 rpm, the rotor displacement along the axis x was 30% of the air gap, and the air gap was assumed to be 1 mm.

In order to determine the reference EMF (voltage U_q), the HSPMG simulation at the zero rotor displacement was conducted. The reference EMF value was 293.43 V. Under the displacement of 30% of the

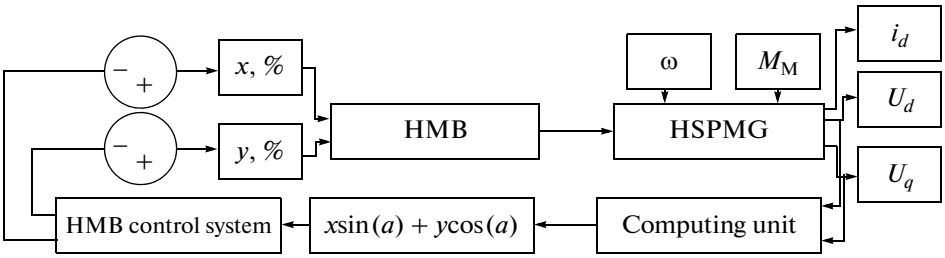

Fig. 4. The simulation model block diagram.

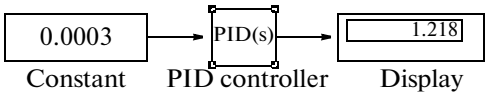

Fig. 5. The implementation of PD controller in *Matlab Simulink*.

air gap, the maximum EMF amplitude was 420 V; then, according to (3.1) $\Delta E_v = 43.13\%$ and taking into account interpolation coefficients determined from (3.2), the eccentricity is

$$\varepsilon = 0.476 \cdot (43.13)^3 - 21.12 \cdot (43.13)^2 + 26.18 \cdot 43.13 + 1.404 \approx 30\%.$$

It follows from (4.1) that the HMB rotor displacement magnitude is determined by

$$y(P1) \approx 0.001 \cdot (0.476 \cdot (43.13)^3 - 21.12 \cdot (43.13)^2 + 26.18 \cdot 43.13 + 1.404) = 0.0003 \text{ m}.$$

The displacement value thus obtained was fed to the input of the PD controller, which was also implemented in Matlab Simulink (Fig. 5). In the simulation, the following parameters of the PD controller were used: $\alpha = 1000$ and $\beta = 40000$. As a result of the simulation, the control current value (1.218 A) was obtained at the PD controller output, which should be then fed to the electromagnet $P1$. After feeding this current to $P1$, the displacement was eliminated, which is clearly illustrated by the proposed control algorithm.

The EMF measurements were made at two rotor rotation angles (0° and 90°, i.e., when $\sin\alpha = 0$ or $\cos\alpha = 0$ in order to determine the displacement along the axes x and y, respectively). This operation was conducted for harmonics 3, 9, and 43 for verification purposes. These operations, as well as the calculation of the interpolation coefficients, were carried out by the computing unit. As a result, the curve for the angle 0° was obtained at the output of the computing unit; its maximum amplitude was equal to the rotor displacement (30%).

Thus, the simulation proved the possibility of the practical implementation of the 5 kW HSPMG rotor position control without rotor position sensors.

CONCLUSIONS

The paper presents a novel method for the sensorless control of HMBs that can also be used to control active magnetic bearings. A mathematical apparatus for its implementation and control algorithm are developed. The proposed algorithm was simulated in *Matlab Simulink* for a high-speed permanent-magnet generator.

The results can be used in practice for the design of electrical machines based on magnetic bearings.

ACKNOWLEDGMENTS

This work was supported by the Ministry of Education and Science of the Russian Federation, project no. 8.287.2014/K

REFERENCES

1. V. E. Vavilov, A. A. Gerasin, and F. R. Ismagilov, "An algorithm for controlling hybrid magnetic bearings using the magnetic field pattern" J. Comput. Syst. Sci. Int., **52**, 794–799 (2013).
2. T. Schuhmann, "Optimale Zustandsschätzung und Regelung an Magnetlagern mit Integriertenmkapazitiven Lagesensoren," PhD Thesis (Technishe Universität, Dresden, 2011).
3. V. Iannello, "Sensor-less position detector for foreign patent documents an active magnetic bearing," US Patent No. 5696412 H02K 7/09, (1997).
4. B. Toshimitsu and T. Yoshida, "Sensorless magnetic bearing apparatus," EP Patent No. 2 083 183 A2 F16C 32/04.2009, (2009).
5. N. G. Nikiyan and M. E. Iondem, "Determining the rotor eccentricity of asynchronous machined given the EMF magnitude of higher harmonics," Izv. Vyssh. Uchebn. Zaved., Elektromekh., No. 11 (1991).
6. A. A. Gerasin, F. R. Ismagilov, I. Kh. Khairullin, et al., "A simulation model of electromechanical energy transformers with regard to processes in bearing assemblies," Sborka v Mashinostroenii, Priborostroenii, No. 2, 35–39 (2013).
7. I. P. Kopylov, *Designing Electrical Machines*, Vol. 1 (Vysshaya shkola, Moscow, 1993) [in Russian].
8. I. N. Bronshtein, *Handbook of Mathematics for Engineers and Students*, 13th ed. (Nauka, Moscow, 1986) [in Russian].
9. B. Heller and V. Hamata, *Harmonic Field Effects in Induction Machines* (Academia, Prague, 1977; Energiya, Moscow, 1981).
10. B. Heller and A. Veverka, *Stosserscheinungen in Elektrischen Maschinen* (VEB Verlag Technik, Berlin, 1957; Gosenergoizdat, Leningrad, 1960).
11. Yu. A. Gaidenko and T. S. Vishnevskii, "A method for electromagnetic diagnosis of the static rotor eccentricity in a synchronous generator," Gidroenergetika Ukrainy, No. 2, 52–57 (2011).
12. A. Sizyakin and M. Rumyantsev, "Doing without rotor position sensor: Solutions of IR company for controlling a brushless electric motor," Novosti Elektroniki, No. 10 (2011).
13. V. E. Vavilov, A. A. Gerasin, and F. R. Ismagilov, "Stability analysis of hybrid magnetic bearings," Syst. Sci. Int., **53**, 130–136 (2014).

Translated by O. Pismenov